Vol. 06, No. 1 (2024) 151-160, doi: 10.24874/PES06.01.017

Proceedings on Engineering Sciences

www.pesjournal.net

# MCS MAP FOR LINK-LEVEL SIMULATION OF TWO-USER PD-NOMA SYSTEM

Yakov Kryukov[1]
Dmitriy Pokamestov
Andrey Brovkin
Artem Shinkevich
Georgiy Shalin

Received 11.02.2023.
Received in revised form 06.07.2023.
Accepted 21.07.2023.
UDC – 004.4`416

Keywords:

*PD-NOMA, NOMA, MCS, SIC*

A B S T R A C T

*Power Domain Non-Orthogonal Multiple Access (PD-NOMA) is a promising technique for future wireless networks. Currently, the growing number of researchers are addressing PD-NOMA issues. The great number of known results are based on the Shannon capacity theorem, assuming infinite code block length. However, they cannot be achieved in practice when modulation and coding schemes (MCS) with finite code block length are used. To solve this problem, we propose an approach which allows utilizing LTE MCSs in the link-level simulation of PD-NOMA. In this paper, we present an adaptive MCS map for a PD-NOMA system with two users, considering non-perfect Serial Interference Cancelation (SIC). In addition, we have developed a map for power allocation coefficients (PAC). The max-sum rate criterion and 10%-Block Error Rate constraint are utilized. The MCS and PAC maps allow access point to jointly and adaptively select MCS parameters for the users depending on their SNR values. The proposed MCS maps can be used in a link-level simulation of the PD-NOMA system to near-practical performance.*



## 1. INTRODUCTION

High standards are imposed on next-generation cellular communication systems, such as Beyond 5G or 6G (Katz et al., 2019). In particular, it is necessary to ensure much higher density of network connections per resource unit and an increase in a channel capacity for the provision of new customer services and applications. Non-orthogonal multiple access (NOMA) can partially satisfy the requirements listed above. NOMA is referred to a group of a large number of techniques. Broadly, all NOMA approaches can be divided into power domain NOMA (PD-NOMA) and code domain NOMA (CD-NOMA). The concept of NOMA is to transmit data of two (or more) users in the same frequency-time resource segment (RS). In orthogonal frequency-division multiplexing (OFDM) systems, RS is an orthogonal subcarrier, so NOMA transmits data from several users on a common subcarrier. Varieties, trends, issues, new approaches, and advantages of NOMA are described in detail in reviews (Abd-Elnaby et al., 2023; Budhiraja et al., 2021).

[1] Corresponding author: Yakov Kryukov
Email: kryukov.tusur@gmail.com

Our work focuses on PD-NOMA that utilizes different power levels for user multiplexing in the power domain (Saito et al., 2013) of an OFDM subcarrier. The total available power is shared between users, and the group signal is formed by the superposition of signals of all users with various power levels from each other. In this case, user channels affect each other, causing inter-channel interference (ICI). One of the main goals of PD-NOMA is ICI management, and it is controlled by two factors: the power allocation (PA) between users and the type of their modulation and coding schemes (MCS).

The goal of PA is to share common power among users by satisfying one of the system criteria (fairness, capacity, latency, energy efficiency, error probability, and so on). Increasing the power share of one of the users allows for increase in its performance, which, at the same time, leads to a decrease in power shares of other users as well as decrease in their performance. Therefore, PA impacts not only the capacity of one user, but also the capacity of other users, and there should be a compromise found.

When performing PA, the main criterion is the channel quality (CQ) of multiplexed users. Fixed PA (FPA) (Benjebbovu et al., 2013) is non-complex, but it does not account for varying CQ. Works (Hojeij et al., 2016; Abd-Elnaby, 2021; El-Sayed et al., 2016) describe low complexity approaches of dynamic PA (DPA) considering varying CQ. They also propose Full Search PA (FSPA) (Benjebbovu et al., 2013) consisting of the enumeration of all possible power levels and the exhaustive search for the optimal solution. As it has a high computational complexity, several FSPA optimization schemes have been proposed (Wu et al., 2021; Alghasmari & Nassef, 2021). The greater number of works, for example (Hojeij et al., 2017; Wang et al., 2016; Xu & Cumanan, 2017; Chen et al., 2018), are devoted to DPA optimization schemes used for maximizing sum-rate and weighted sum-rate. Some researchers put forward various schemes (Liu et al., 2015; Fu et al., 2018; 17. Al-Abbasi & So, 2016; Dogra & Bharti, 2022; Mei et al., 2016; Wang et al., 2019) concerning the joint user pairing and PA (UPPA), mostly focused on addressing optimization problems. All of the above studies are based on the Shannon capacity formula ignoring the bit error rates (BERs) of PD-NOMA users. Hence, they focus only on achievable rates (capacity region) without considering the problem of error propagation of co-allocated users.

The MCS selection in PD-NOMA and OMA is not identical and also allows for the ICI management. The common constellation is obtained by the superposition of several users' constellations (mostly QAM) with various power levels. Increasing the modulation order of one user leads to a decrease in the Euclidean distance between the constellation points of other users and increases error probability. In particular, (Iraqi & Al-Dweik, 2021; Ferdi & Hakan, 2020; Cejudo et al., 2017; Choi, 2016) address the problem of PA considering QAM.

The PA and MCS selection are solved together because they are interrelated. There is the sufficient number of papers devoted to this issue. Among them, a number of works solve the issue using the iterative search, which is computationally complex (Kim et al., 2018; Cejudo et al., 2021; Yu et al., 2021). In addition, several papers use assumptions that reduce the accuracy of results. The authors Kim et al. (2018) assume perfect serial interference cancellation (SIC), which is a simplification that reduces accuracy. In (Cejudo et al., 2021), the researchers perform constant BER but they use an approximation to calculate it. The QAM modulation and power adaptation for downlink two-user PD-NOMA are studied in (Yu et al., 2021). The proposed algorithms make it possible to select the QAM order and PA without exceeding a given BER threshold. The paper is of considerable interest; however, it uses an iterative search approach and considers conventional QAM, not MSCs.

Another approach of the PA and MCS selection is to construct a ready-made adaptive map with pre-calculated multiplexing settings. The benefit of this approach is that optimal settings can be defined in advance, eliminating the need for the real-time iterative search. In (Hsieh et al., 2016), the authors describe their own approach for constructing the MCS map for co-allocated users assuming symbol level SIC (SL-SIC). To build such an MCS map, the first step is to find BERs of co-allocated users with given SNRs, MCS settings, and PACs. Using the exhaustive search in a simulation model, the authors determine the feasibility of assigning any given pairwise combination of MCS (8 MCSs pool) and PAC to data transfer under given SNR (from 15 to 50 dB), while ensuring that BERs do not exceed $10^{-4}$ for each user. Next, all feasible combinations are recorded in the MCS map.

In (Thieu et al., 2017, Yang & Hsieh, 2015), the authors present the MCS map using the following method. It is constructed similar to the method employed in (Hsieh et al., 2016), recording the combination of PA coefficients (PACs) and MCSs (10 MCSs pool) that satisfy the BER threshold constraint $10^{-4}$ for co-allocated users within the given SNR range of 4 to 22 dB. At the receiver side, the SL-SIC is implemented.

Other researchers (Endovitskiy et al., 2021) present the PA and MCS selection while analyzing the performance of downlink PD-NOMA in Wi-Fi networks. To solve these problems, the signal-to-noise and interference ratio (SINR) for two users is obtained, incorporating the ICI component from the second user as additive white Gaussian noise (AWGN). Further, the pair of MCSs with the performance exceeding the SINR threshold is selected from the table. The disadvantage of such an approach is that taking ICI as AWGN is a simplification

and gives additional inaccuracy in the data receiving quality metrics (BER, BLER, etc.).

In contrast to related works, we propose an approach for constructing maps for the adaptive joint MCS selection and PA for non-perfect SIC, considering 10% BLER fulfillment. To prove it, we present two maps for SL-SIC and codeword level SIC (CWL-SIC) with 1 dB SNR resolution. Furthermore, we demonstrate the performance of the system with CWL-SIC compared to SL-SIC and show that CWL-SIC outperforms SL-SIC under poor channel conditions. Future studies can utilize these maps for the link-level simulation of PD-NOMA systems and obtain more practical system performance.

## 2. SYSTEM MODEL

### 2.1 Downlink PD-NOMA signal

We consider a basic downlink PD-NOMA scenario where an access point (AP) serves two users. User 1 is located at the cell edge and possesses a "weak" propagation channel, and user 2 is located close to AP and possesses a "strong" propagation channel. The data from both users is transmitted on the common orthogonal subcarrier by multiplexing in the power domain with different PACs $\mathbf{p} = \{p_1, p_2\}$, where $p_k$ is assigned to user $k \in \{1,2\}$, fulfilling $p_1 > p_2$ and $p_1 + p_2 = 1$. The data transfer is conducted using a set of MCSs, the settings of which are shown in Fig.1. Let us denote the data symbols of user 1 and user 2 by variables $x \in \mathbf{X}, y \in \mathbf{Y}$, where $\mathbf{X}$, $\mathbf{Y}$ represent the QAM alphabet determined by the modulation orders $\mathbf{Q} = \{Q_1, Q_2\}$ of MCSs. Thus, the group PD-NOMA symbol $s$ to be transmitted on the subcarrier is given by

$$s = \sqrt{p_1}x + \sqrt{p_2}y. \quad (1)$$

### 2.2 SL-SIC

The received signals at user $k$ are expressed as

$$r_k = \alpha_k s + n_k, \quad (2)$$

where $n_k \sim \mathcal{CN}(0, \sigma^2)$ is the noise realization of user $k$ with zero mean and variance $\sigma^2$, and $\alpha_k$ is the channel coefficient from AP to user $k$.

Let us consider the process of SL-SIC decoding in the AWGN channel. At the receiver of user 1, its own $\hat{x}$ is estimated using the minimum Euclidean distance criterion, treating the signal from user 2, $\sqrt{p_2}y$, as interference according to

$$\hat{x} = \arg\min_{x_i \in \mathbf{X}} \left| \sqrt{p_1}(x - x_i) + \sqrt{p_2}y + \frac{n_1}{\alpha_1} \right|^2. \quad (3)$$

At the receiver of user 2, $\hat{x}$ is first decoded according to (3), replacing $\frac{n_1}{\alpha_1}$ by $\frac{n_2}{\alpha_2}$. SL-SIC does not use forward error correction (FEC) codes, hence the cancelation signal $\sqrt{p_1}x^*$ is generated directly from $\hat{x}$ at the symbol level, and $x^* = \hat{x}$. Next, $\sqrt{p_1}x^*$ is removed from the received signal and then user 2 obtains its own $\hat{y}$ as follows:

$$\hat{y} = \arg\min_{y_i \in \mathbf{Y}} \left| \sqrt{p_1}(x - x^*) + \sqrt{p_2}(y - y_i) + \frac{n}{\alpha_2} \right|^2. \quad (4)$$

PD-NOMA researchers often consider perfect SIC, wherein interference component $x^*$ is canceled perfectly, leading to a revised form of equation (4):

$$\hat{y} = \arg\min_{y_i \in \mathbf{Y}} \left| \sqrt{p_2}(y - y_i) + \frac{n}{\alpha_2} \right|^2. \quad (5)$$

Perfect SIC is fairly considered when the error probability of $\hat{x}$ is significantly lower than that of $\hat{y}$. It is assumed that $s$ is formed in such a way that $\hat{x}$ is decoded without errors at the receiver of user 2, which may reduce the system capacity as well as the PA and MCS selection range. In addition, the system models with perfect SIC cannot provide an accurate measure of system performance that depends on the data reception metric (e.g., BER). More correctly, we consider a system with non-perfect SIC, and CWL-SIC can be utilized to improve the quality of the cancelation signal.

### 2.3 CWL-SIC

Now let us consider CWL-SIC that can only be performed at the receiver of user 2. Compared to SL-SIC, CWL-SIC employs FEC, thereby reducing the probability of error cancelation in (4) and bringing the received $\hat{y}$ closer to perfect SIC (5). However, it increases the computational complexity due to the need for encoding/decoding of the external signal.

In CWL-SIC, $x^*$ is carried out in several successive stages: a) obtaining $\hat{x}$ (3); b) FEC decoding $\hat{x}$, correcting errors and coding again; c) $Q_1$-QAM mapping of the codeword and obtaining $x^*$. CWL-SIC gives the BER benefit of $\hat{y}$ under poor CQ, when there is a high error probability of $\hat{x}$ at the receiver of user 2.

## 3. CONSTRUCTION OF MCS MAPS

### 3.1 MCS characteristics

We have utilized the MCS table from the LTE standard in our paper. It contains $M = 15$ schemes (Fig. 1), each of which is characterized by the following parameters: $m$ — MCS index; $Q$ — QAM order; $\gamma/1024$ — code rate (Turbo); $Z$ — SNR threshold that provides 10% BLER; and $\rho^z$ — BER at the decoder input under $Z$ conditions. The SNR thresholds are specified by the performance of the decoding algorithm provided in (Fan et al., 2011).

| $m$ | $Q$ | $\gamma/1024$ | $R$ bits/symb | $Z$, dB SNR Threshold | $\rho^z$ BER at the decoder input | BLER at the decoder output |
|---|---|---|---|---|---|---|
| 1 | 4 | 78 | 0.1523 | -9.478 | 0.368551 | 10% |
| 2 | 4 | 120 | 0.2344 | -6.658 | 0.320891 | |
| 3 | 4 | 193 | 0.3770 | -4.098 | 0.266385 | |
| 4 | 4 | 308 | 0.6010 | -1.798 | 0.208131 | |
| 5 | 4 | 449 | 0.8770 | 0.399 | 0.147637 | |
| 6 | 4 | 602 | 1.1758 | 2.424 | 0.093168 | |
| 7 | 16 | 378 | 1.4766 | 4.489 | 0.177906 | |
| 8 | 16 | 490 | 1.9141 | 6.367 | 0.135497 | |
| 9 | 16 | 616 | 2.4063 | 8.456 | 0.090319 | |
| 10 | 64 | 466 | 2.7305 | 10.266 | 0.147952 | |
| 11 | 64 | 567 | 3.3223 | 12.218 | 0.111380 | |
| 12 | 64 | 666 | 3.9023 | 14.122 | 0.078752 | |
| 13 | 64 | 772 | 4.5234 | 15.849 | 0.051696 | |
| 14 | 64 | 873 | 5.1152 | 17.786 | 0.026572 | |
| 15 | 64 | 948 | 5.5547 | 19.809 | 0.009611 | |

**Figure 1.** MCS table from LTE standard

## 3.2 Pairwise MCS combinations

In the initial step, we construct all possible pairwise MCS combinations $\{m_1, m_2\}$ using the MCS table (Fig. 1), where $m_k$ is assigned to user $k$. We assume that assigning a higher data rate to user 1 compared to user 2 is not reasonable due to the worse channel condition of user 2,
since it is not efficient for the system. Therefore, we exclude combinations where $m_1 > m_2$ from the composed pairwise combinations and obtain $J = 120$ combinations sorted in ascending order of total data rate $R_\Sigma(j) = R_{m_1}(j) + R_{m_2}(j)$, where $j \in 1 \dots J$ is a combination index. All the composed combinations are shown in Fig. 2.

## 3.3 Algorithm of MCS map construction

When constructing the MCS map, the goal is to find (via enumeration) the index $l \in 1 \dots J$ of the combination with the highest data rate $R_\Sigma$ under pairwise SNR condition $\mathbf{W} = \{W_1, W_2\}$. This choice is to ensure that the error probability does not exceed 10% BLER when decoding $\hat{x}, \hat{y}$. We define the SNR of user $k$ as $W_k = \frac{|\alpha_k|^2}{\sigma^2}$.

For the BLER condition to be satisfied, it is sufficient that BER is lower than the threshold value $\rho^z$ (Fig. 1). The search of $l$ can be expressed as follows

$$l = max_{j \in 1 \dots J} R_\Sigma(j), \tag{6}$$

fulfilling that

$$\begin{cases} \rho_{\hat{x}}(\boldsymbol{m}(j), \boldsymbol{p}, W_1) \le \rho^z\big(m_1(j)\big) \\ \rho_{\hat{y}}(\boldsymbol{m}(j), \boldsymbol{p}, W_2) \le \rho^z\big(m_2(j)\big) \end{cases}, \tag{7}$$

where $\rho_{\hat{x}}(\mathbf{m}(j), \mathbf{p}, W_1)$ and $\rho_{\hat{y}}(\mathbf{m}(j), \mathbf{p}, W_2)$ are BERs of $\hat{x}$ and $\hat{y}$, where $\mathbf{m}(j) = \{m_1(j), m_2(j)\}$ contains MCS indices of the $j$-th combination (Fig. 2); $\mathbf{p}$ contains PACs; $\rho^z\big(m_k(j)\big)$ is the BER threshold of $m_k(j)$.

## 3.4 BER calculation

BER on SNR is calculated using the exact expressions derived in (Assaf et al., 2020), depending on specific PD-NOMA signal settings such as $\mathbf{Q}$ and $\mathbf{p}$. In turn, $\mathbf{Q}$ is defined by the MCS $\mathbf{m}(j)$ of $j$-th combination, and the exhaustive search is used to set $\mathbf{p}$, which is described in the next section. Thus, for the non-perfect SL-SIC receiver, $\rho_{\hat{x}}(\mathbf{m}(j), \mathbf{p}, W_1)$ and $\rho_{\hat{y}}(\mathbf{m}(j), \mathbf{p}, W_2)$ can be obtained by (14) and (20) from (Assaf et al., 2020), respectively.

In CWL-SIC, $\rho_{\hat{x}}(\mathbf{m}(j), \mathbf{p}, W_1)$ is obtained in the same manner as in SL-SIC, utilizing (14) from (Assaf et al., 2020). Now, let us describe $\rho_{\hat{y}}(\mathbf{m}(j), \mathbf{p}, W_2)$ in CWL-SIC and note two situations that occur when demodulating $\hat{x}$ at the receiver of user 2 under SNR condition $W_2$.

1) The strong user 1 signal at the receiver of user 2, satisfying $\rho_{\hat{x}}(\mathbf{m}(j), \mathbf{p}, W_2) \le \rho^z\big(m_1(j)\big)$. Because of the strong reception and fulfillment of 10% BLER, we assume that all bit errors in $x^*$ are corrected, enabling perfect SIC. Then, the signal after cancelation is $\sqrt{p_2}y + n$, which is weighted by the $p_2$ symbol of $Q_2$-QAM superposed with noise component $n$. In this case, $\rho_{\hat{y}}(\mathbf{m}(j), \mathbf{p}, W_2)$ is calculated as for conventional QAM (eq. (16) from (Cho & Yoon, 2002), using $\gamma = W_2 p_2 / \log_2 Q_2$).

2) The weak user 1 signal at the user 2 receiver, satisfying $\rho_{\hat{x}}(\mathbf{m}(j), \mathbf{p}, W_2) > \rho^z\big(m_1(j)\big)$. High $\rho_{\hat{x}}$ does not allow the decoder to correct errors in $x^*$, which is non-perfectly removed from the received signal. In this case, $\rho_{\hat{y}}(\mathbf{m}(j), \mathbf{p}, W_2)$ is calculated as for non-perfect SIC by (20) from (Assaf et al., 2020).

| $j$ | $m_1$ | $m_2$ | $R_\Sigma$ | $j$ | $m_1$ | $m_2$ | $R_\Sigma$ | $j$ | $m_1$ | $m_2$ | $R_\Sigma$ | $j$ | $m_1$ | $m_2$ | $R_\Sigma$ | $j$ | $m_1$ | $m_2$ | $R_\Sigma$ | $j$ | $m_1$ | $m_2$ | $R_\Sigma$ |
|---|---|---|---|---|---|---|---|---|---|---|---|---|---|---|---|---|---|---|---|---|---|---|---|
| 1 | 1 | 1 | 0.3046 | 21 | 4 | 6 | 1.7774 | 41 | 3 | 10 | 3.1075 | 61 | 4 | 12 | 4.5039 | 81 | 4 | 14 | 5.7168 | 101 | 11 | 12 | 7.2246 |
| 2 | 1 | 2 | 0.3867 | 22 | 3 | 7 | 1.8536 | 42 | 5 | 9 | 3.2833 | 62 | 8 | 10 | 4.6446 | 82 | 9 | 11 | 5.7286 | 102 | 10 | 13 | 7.2539 |
| 3 | 2 | 2 | 0.4688 | 23 | 5 | 6 | 2.0528 | 43 | 4 | 10 | 3.3321 | 63 | 1 | 13 | 4.6757 | 83 | 2 | 15 | 5.7891 | 103 | 8 | 15 | 7.4688 |
| 4 | 1 | 3 | 0.5293 | 24 | 1 | 8 | 2.0664 | 44 | 7 | 8 | 3.3907 | 64 | 2 | 13 | 4.7578 | 84 | 8 | 12 | 5.8164 | 104 | 9 | 14 | 7.5215 |
| 5 | 2 | 3 | 0.6114 | 25 | 4 | 7 | 2.0782 | 45 | 1 | 11 | 3.4746 | 65 | 5 | 12 | 4.7793 | 85 | 3 | 15 | 5.9317 | 105 | 12 | 12 | 7.8046 |
| 6 | 1 | 4 | 0.7539 | 26 | 2 | 8 | 2.1485 | 46 | 2 | 11 | 3.5567 | 66 | 7 | 11 | 4.7989 | 86 | 5 | 14 | 5.9922 | 106 | 11 | 13 | 7.8457 |
| 7 | 3 | 3 | 0.7540 | 27 | 3 | 8 | 2.2911 | 47 | 6 | 9 | 3.5821 | 67 | 9 | 9 | 4.8126 | 87 | 7 | 13 | 6 | 107 | 10 | 14 | 7.8457 |
| 8 | 2 | 4 | 0.8360 | 28 | 6 | 6 | 2.3516 | 48 | 5 | 10 | 3.6075 | 68 | 3 | 13 | 4.9004 | 88 | 10 | 11 | 6.0528 | 108 | 9 | 15 | 7.9610 |
| 9 | 3 | 4 | 0.9786 | 29 | 5 | 7 | 2.3536 | 49 | 3 | 11 | 3.6993 | 69 | 6 | 12 | 5.0781 | 89 | 4 | 15 | 6.1563 | 109 | 10 | 15 | 8.2852 |
| 10 | 1 | 5 | 1.0293 | 30 | 4 | 8 | 2.5157 | 50 | 8 | 8 | 3.8282 | 70 | 4 | 13 | 5.1250 | 90 | 6 | 14 | 6.2910 | 110 | 12 | 13 | 8.4257 |
| 11 | 2 | 5 | 1.1114 | 31 | 1 | 9 | 2.5586 | 51 | 7 | 9 | 3.8829 | 71 | 9 | 10 | 5.1368 | 91 | 9 | 12 | 6.3086 | 111 | 11 | 14 | 8.4375 |
| 12 | 4 | 4 | 1.2032 | 32 | 2 | 9 | 2.6407 | 52 | 6 | 10 | 3.9063 | 72 | 8 | 11 | 5.2364 | 92 | 5 | 15 | 6.4317 | 112 | 11 | 15 | 8.8770 |
| 13 | 3 | 5 | 1.2540 | 33 | 6 | 7 | 2.6524 | 53 | 4 | 11 | 3.9239 | 73 | 1 | 14 | 5.2675 | 93 | 8 | 13 | 6.4375 | 113 | 12 | 14 | 9.0175 |
| 14 | 1 | 6 | 1.3281 | 34 | 3 | 9 | 2.7833 | 54 | 1 | 12 | 4.0546 | 74 | 2 | 14 | 5.3496 | 94 | 7 | 14 | 6.5918 | 114 | 13 | 13 | 9.0468 |
| 15 | 2 | 6 | 1.4102 | 35 | 5 | 8 | 2.7911 | 55 | 2 | 12 | 4.1367 | 75 | 7 | 12 | 5.3789 | 95 | 10 | 12 | 6.6328 | 115 | 12 | 15 | 9.4570 |
| 16 | 4 | 5 | 1.4786 | 36 | 1 | 10 | 2.8828 | 56 | 5 | 11 | 4.1993 | 76 | 5 | 13 | 5.4004 | 96 | 11 | 11 | 6.6446 | 116 | 13 | 14 | 9.6386 |
| 17 | 3 | 6 | 1.5528 | 37 | 7 | 7 | 2.9532 | 57 | 7 | 10 | 4.2071 | 77 | 10 | 10 | 5.4610 | 97 | 6 | 15 | 6.7305 | 117 | 13 | 15 | 10.078 |
| 18 | 1 | 7 | 1.6289 | 38 | 2 | 10 | 2.9649 | 58 | 3 | 12 | 4.2793 | 78 | 3 | 14 | 5.4922 | 98 | 9 | 13 | 6.9297 | 118 | 14 | 14 | 10.2304 |
| 19 | 2 | 7 | 1.7110 | 39 | 4 | 9 | 3.0079 | 59 | 8 | 9 | 4.3204 | 79 | 6 | 13 | 5.6992 | 99 | 8 | 14 | 7.0293 | 119 | 14 | 15 | 10.6699 |
| 20 | 5 | 5 | 1.7540 | 40 | 6 | 8 | 3.0899 | 60 | 6 | 11 | 4.4981 | 80 | 1 | 15 | 5.7070 | 100 | 7 | 15 | 7.0313 | 120 | 15 | 15 | 11.1094 |

**Figure 2.** Pairwise MCSs combinations

### 3.5 Exhaustive search of PACs

The exploitation of QAM imposes a restriction on the ratio between PACs. Violating this restriction causes the constellation of user 2 to extend beyond the boundaries of the decoding region of the constellation of user 1 (constellation overlap) and results in a significant increase of $\rho_{\hat{x}}$. To avoid this, we use constrain on $\mathbf{p}$ described in (Kryukov et al., 2023). For given modulation orders $\mathbf{Q}$, the restriction on $\mathbf{p}$ will be the following:

$$\begin{cases} p_1^{min} \le p_1 < 1 \\ 0 < p_2 \le 1 - p_1^{min} \end{cases}, \tag{8}$$

where $p_1^{min}$ is minimum PAC assigned to user 1, ensuring that there will be no constellation overlap, and it can be obtained by

$$p_1^{min} = \frac{\left(\sqrt{Q_2} - 1\right)(Q_1 - 1)}{Q_1\left(\sqrt{Q_2} - 1\right) + 2}. \tag{9}$$

When performing the exhaustive search, for each combination $\mathbf{m}(j)$ under condition $\mathbf{W}$, we search $\mathbf{p}$ in the range (8) that satisfies (7). If no such $\mathbf{p}$ is found, then $j$-th combination cannot be selected for data transmission under conditions $\mathbf{W}$. We use search resolution $\Delta p_1$ as follow

$$\Delta p_1 = \frac{1 - p_1^{min}}{d}, \tag{10}$$

where $d$ is the search accuracy, which linearly splits the search range $[p_1^{min}, 1)$ into $d$ valid values, reducing the computational complexity.

## 4. MCS MAPS FOR SL-SIC AND CWL-SIC

### 4.1 MCS maps

Fig. 3 shows the proposed adaptive MCS map for two-user PD-NOMA with non-perfect SL-SIC. It is obtained for the SNR range of -10 to 40 dB with 1 dB resolution. Under SNR conditions $\mathbf{W}$, AP selects the $j(\mathbf{W})$ number of a combination containing MCS indices $\mathbf{m}(j)$ for both users. The color grading shows the total data rate $R_\Sigma(\mathbf{W})$, and $\max(R_\Sigma) = 11.1094$ bits per subcarrier is reached by $j = 120$ combination in a high SNR region.

Jointly with $j(\mathbf{W})$, AP selects the corresponding parameter $i(\mathbf{W})$, which is involved in the calculation of $\mathbf{p}$ according to

$$\begin{cases} p_1 = p_1^{min} + (i-1) \cdot \Delta p_1 \\ p_2 = 1 - p_1 \end{cases},$$

where $p_1^{min}$ and $\Delta p_1$ are obtained by (8, 9) depending on $\mathbf{Q} \in \mathbf{m}(j)$. Fig. 4 shows the mapping of $i$ obtained by the exhaustive search using $d = 16$.

Fig. 5 shows the proposed adaptive MCS map for CWL-SIC decoding and Fig. 6 summarizes PACs. The parameters and algorithm of this map are identical for both cases.

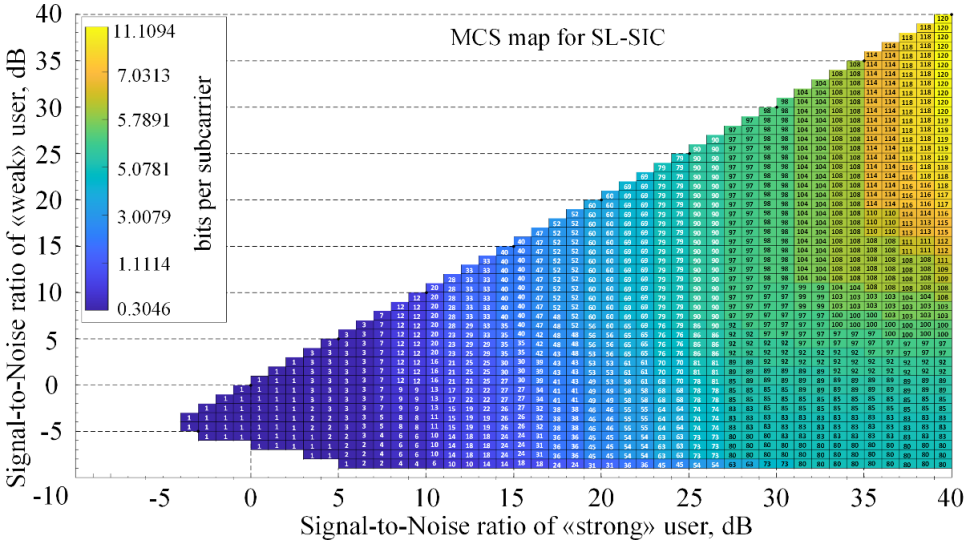


**Figure 3.** MCS map for SL-SIC

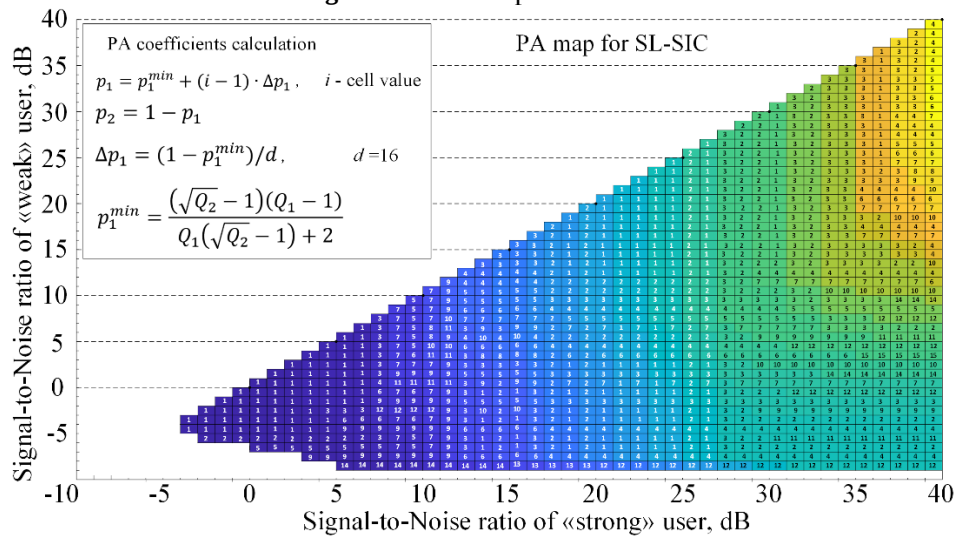


**Figure 4.** PA map for SL-SIC

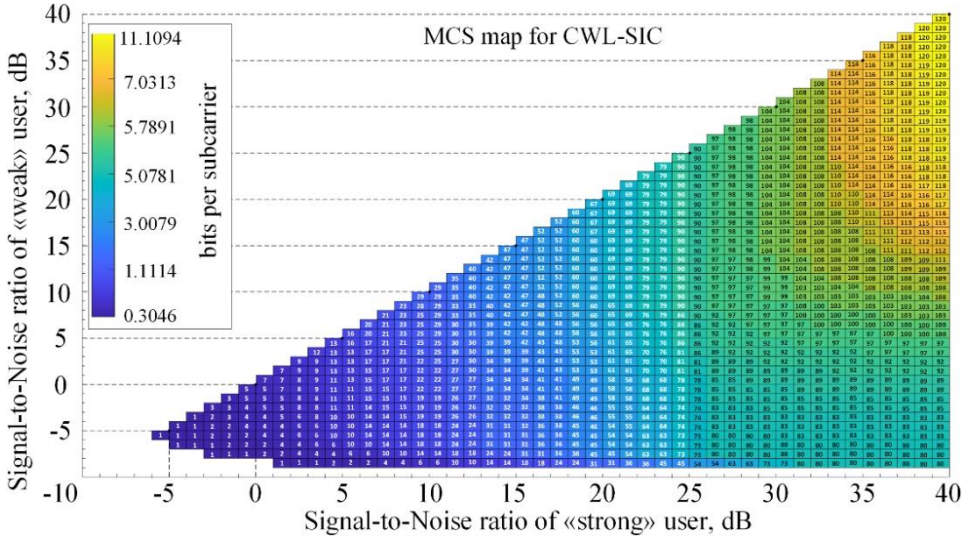


**Figure 5.** MCS map for CWL-SIC

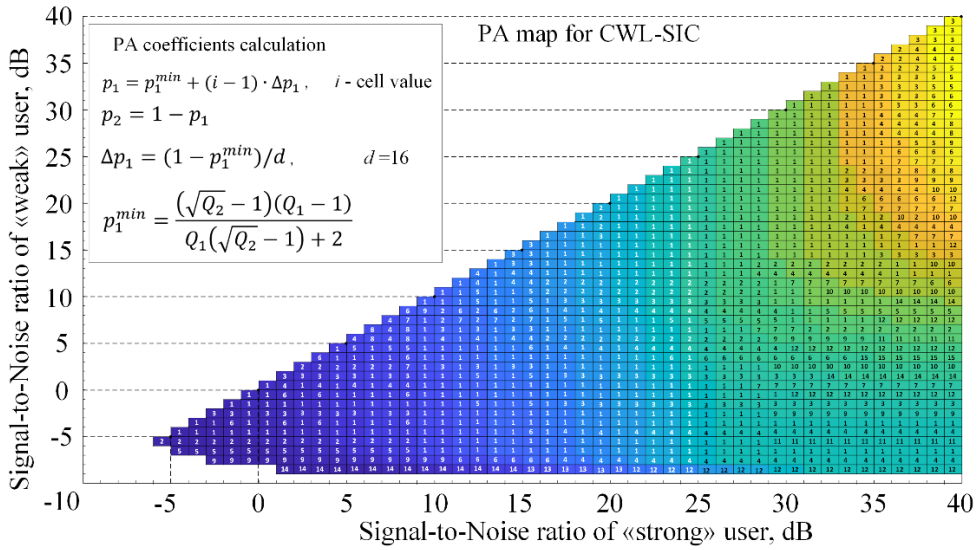


**Figure 6.** PA map for CWL-SIC

## 4.2 Comparison of SL-SIC and CWL-SIC

Fig. 7 shows the benefit of CWL-SIC relative to SL-SIC. Thus, the figure shows a region where CWL-SIC allows for the data transmission while SL-SIC is unable to make it feasible. This region is marked by the red color. It is seen that CWL-SIC moves the SNR threshold to a lower region, allowing for the data transmission at worse SNR than what is achievable with SL-SIC.

Thus, CWL-SIC provides benefit in the low SNR region when both users have poor CQ. The area with high gain is highlighted in a bright color, and the area with low gain is shown in dark blue. The numerical gain can be up to 270% in the low SNR region and it varies from 0 to 10% in the high SNR region. The obtained result shows the feasibility of CWL-SIC as a means to increase the capacity of the PD-NOMA system, despite the increased computational complexity due to the additional decoding-encoding process.

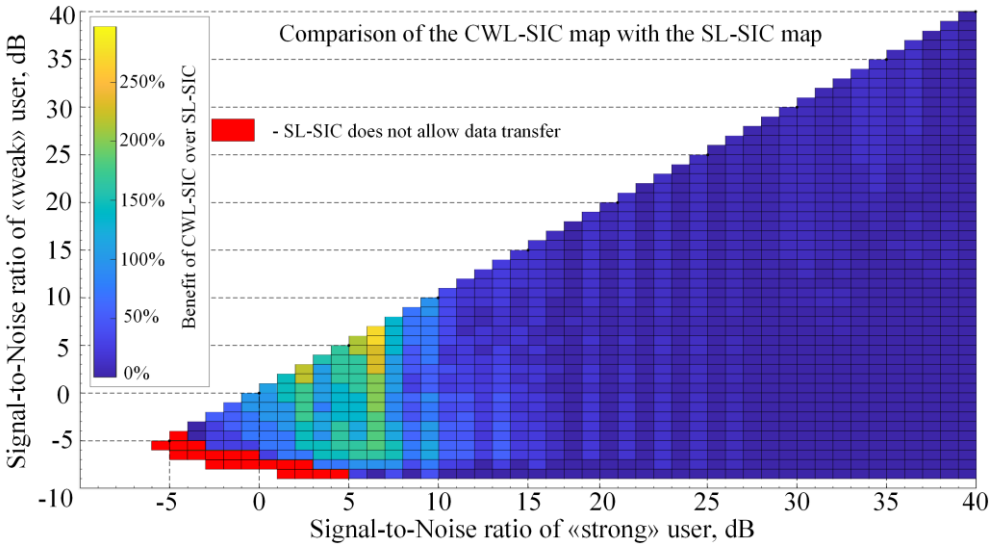


**Figure 7.** Comparison of SL-SIC and CWL-SIC

## 5. CONCLUSION

The paper presents a method for constructing the MCS map for a two-user PD-NOMA system. It allows for considering the performance of real MCSs in the link-level simulations of PD-NOMA. The map uses the strategy of maximizing the total data rate without exceeding the 10% BLER threshold.

Adaptive MCS and PA maps for SL-SIC and CWL-SIC have been proposed. They are obtained for the SNR range of -10 to 40 dB with 1 dB resolution. MCSs from the LTE standard are employed. For the specified user SNR values, the MCS map allows AP to select the optimal MCS pairwise combination settings for PD-

NOMA multiplexing. The PA map is used jointly with the MCS map and enables PA between users.

The comparison of MCS maps for SL-SIC and CWL-SIC is obtained. CWL-SIC demonstrates advantages in a low SNR region when both users have poor channel quality. The result shows the feasibility of CWL-SIC as a means to increase the capacity of the PD-NOMA system.

**Acknowledgement:** The work was supported by the Russian Science Foundation within the framework of 2022 competition "Conducting Research by Research Groups Led by Young Scientists" of the Presidential Program of Research Projects Implemented by Leading Scientists, including Young Scientists. Project No. 22-79-10148.

## References:

Abd-Elnaby, M. (2021). Capacity and fairness maximization-based resource allocation for downlink NOMA networks. *Computers, Materials & Continua*, *69*(1), 521-537. doi: 10.32604/cmc.2021.018351

Abd-Elnaby, M., Sedhom, G., El-Rabaie, E., & Elwekeil, M. (2023). NOMA for 5G and beyond: literature review and novel trends. *Wireless Networks*, *29*(4), 1629-1653. doi: 10.1007/s11276-022-03175-7

Al-Abbasi, Z., & So, D. (2016). User-pairing based non-orthogonal multiple access system. In 2016 IEEE 83rd vehicular technology conference (VTC Spring), pp. 1-5

Alghasmari, W. F., & Nassef, L. (2021). Optimal power allocation in downlink non-orthogonal multiple access (NOMA). *International Journal of Advanced Computer Science and Applications*, *12*(2), 318-325. doi: 10.14569/IJACSA.2021.0120240

Assaf, T., Al-Dweik, A., El Moursi, M., Zeineldin, H., & Al-Jarrah, M. (2020). Exact bit error-rate analysis of two-user NOMA using QAM with arbitrary modulation orders. *IEEE Communications Letters*, vol. 24, no. 12, pp. 2705–2709. doi: 10.1109/LCOMM.2020.3020161

Benjebbovu, A., Li, A., Saito, Y., Kishiyama, Y., Harada, A., & Nakamura, T. (2013). System-level performance of downlink NOMA for future LTE enhancements. *In 2013 IEEE Globecom workshops (GC Wkshps)*, pp. 66-70. doi: 10.1109/GLOCOMW.2013.6824963

Budhiraja, I., Kumar, N., Tyagi, S., Tanwar, S., Han, Z., Piran, M. J., & Suh, D. Y. (2021). A systematic review on NOMA variants for 5G and beyond. *IEEE Access*, *9*, 85573-85644. doi: 10.1109/ACCESS.2021.3081601

Cejudo, E. C., Zhu, H., & Wang, J. (2021). Resource allocation in multicarrier NOMA systems based on optimal channel gain ratios. *IEEE Transactions on Wireless Communications*, vol. 21, no. 1, pp. 635–650. doi: 10.1109/TWC.2021.3098572

Cejudo, E., Zhu, H., & Alluhaibi, O. (2017). On the power allocation and constellation selection in downlink NOMA. In *IEEE 86th Vehicular Technology Conference (VTC-Fall)*, pp. 1–5. doi: 10.1109/VTCFall.2017.8288077

Chen, R., Wang, X., & Xu, Y. (2018). Power allocation optimization in MC-NOMA systems for maximizing weighted sumrate. In *2018 24th Asia-Pacific Conference on Communications (APCC)*, pp. 392–396. doi: 10.1109/APCC.2018.8633549

Cho, K., & Yoon, D. (2002). On the general BER expression of one-and two-dimensional amplitude modulations. *IEEE Transactions on Communications*, vol. 50, no. 7, pp. 1074–1080. doi: 10.1109/TCOMM.2002.800818

Choi, J. (2016). On the power allocation for a practical multiuser superposition scheme in NOMA systems. *IEEE Communications Letters*, *20*(3), 438-441. doi: 10.1109/LCOMM.2016.2518165

Dogra, T., & Bharti, M. R. (2022). User pairing and power allocation strategies for downlink NOMA-based VLC systems: An overview. *AEU-International Journal of Electronics and Communications*, *149*, pp. 154184. doi: 10.1016/j.aeue.2022.154184

El-Sayed, M. M., Ibrahim, A. S., and Khairy, M. M. (2016). Power allocation strategies for non-orthogonal multiple access. In *2016 International Conference on Selected Topics in Mobile & Wireless Networking (MoWNeT)*, pp. 1–6. doi: 10.1109/MoWNet.2016.7496633

Endovitskiy, E., Kureev, A., Levitsky, I., Tutelian, S., & Khorov, E. (2021). Performance evaluation of downlink non-orthogonal multiple access in Wi-Fi networks. *Journal of Communications Technology and Electronics*, vol. 66, pp. 1485–1490. doi: 10.1134/S106422692112007X

Fan, J., Yin, Q., Li, G. Y., Peng, B., & Zhu, X. (2011). MCS selection for throughput improvement in downlink LTE systems. In *2011 Proceedings of 20th international conference on computer communications and networks (ICCCN)*, pp. 1-5. doi: 10.1109/ICCCN.2011.6005743

Ferdi, K., & Hakan, K., (2020). A true power allocation constraint for non-orthogonal multiple access with M-QAM signalling. In *2020 IEEE Microwave Theory and Techniques in Wireless Communications (MTTW)*, vol. 1, pp. 7-12. doi: 10.1109/MTTW51045.2020.9245060

Fu, Y., Salaun, L., Sung, C., & Chen, C. (2018). Subcarrier and power allocation for the downlink of multicarrier NOMA systems. *IEEE Transactions on Wireless Communications*, *67*(12), 11833-11847. doi: 10.1109/TVT.2018.2875601

Hojeij, M. R., Farah, J., Nour, C. A., & Douillard, C. (2016). New optimal and suboptimal resource allocation techniques for downlink non-orthogonal multiple access. *Wireless Personal Communication*, *87*(3), 837-867. doi: 10.1007/s11277-015-2629-2

Hojeij, M., Abdel Nour, C., Farah, J., & Douillard, C. (2017). Waterfilling-based proportional fairness scheduler for downlink non-orthogonal multiple access. *IEEE Wireless Communications Letters*, 6(2), 230-233

Hsieh, H., Yang, M., & Wang, C. (2016). Fair resource allocation using the MCS map for multi-user superposition transmission (MUST). In *2016 IEEE 27th Annual International Symposium on Personal, Indoor, and Mobile Radio Communications (PIMRC)*, pp. 1-7. doi: 10.1109/PIMRC.2016.7794796

Iraqi, Y., & Al-Dweik, A. (2021). Power allocation for reliable SIC detection of rectangular QAM-based NOMA systems. *IEEE Transactions on Vehicular Technology*, *70*(8), 8355-8360. doi: 10.1109/TVT.2021.3096648

Katz, M., Pirinen, P., & Posti, H. (2019). Towards 6G: Getting ready for the next decade. *16th International Symposium on Wireless Communication Systems (ISWCS)*, pp. 714-718. doi: 10.1109/ISWCS.2019.8877155

Kim, S., Kim, H., & Hong, D. (2018). Joint power allocation and MCS selection in downlink NOMA system. In *2018 IEEE 29th Annual International Symposium on Personal, Indoor and Mobile Radio Communications (PIMRC)*, pp. 1-4. doi: 10.1109/PIMRC.2018.8580995

Kryukov, Y. V., Pokamestov, D. A., & Rogozhnikov, E. V. (2023). Comparison of Theoretical and Real Throughput of PD-NOMA. *Journal of Communications Technology and Electronics*, vol. 68, no. 1, pp. 88–95. doi: 10.1134/S1064226922120117

Liu, F., Mahonen, P., & Petrova, M. (2015). Proportional fairness-based user pairing and power allocation for nonorthogonal multiple access. In *IEEE 26th Annual International Symposium on Personal, Indoor, and Mobile Radio Communications (PIMRC)*, pp. 1127–1131. doi: 10.1109/PIMRC.2015.7343467

Mei, J., Yao, L., Long, H., & Zheng, K. (2016). Joint user pairing and power allocation for downlink non-orthogonal multiple access systems. In *2016 IEEE International Conference on Communications (ICC)*, pp. 1–6. doi: 10.1109/ICC.2016.7510914

Saito, Y., Kishiyama, Y., Benjebbour, A., Nakamura, T., Li, A., & Higuchi, K. (2013). Non-orthogonal multiple access (NOMA) for cellular future radio access. *In 2013 IEEE 77th vehicular technology conference (VTC Spring)*, pp. 1-5. doi: 10.1109/VTCSpring.2013.6692652

Thieu, Q., Wang, C., Wang, C., & Hsieh, H. Y. (2017). Design and implementation of NOMA subband scheduling towards larger bandwidth beyond LTE-A. In *IEEE 28th Annual International Symposium on Personal, Indoor, and Mobile Radio Communications (PIMRC)*, pp. 1–7. doi: 10.1109/PIMRC.2017.8292766

Wang, C., Chen, J., & Chen, Y. (2016). Power allocation for a downlink non-orthogonal multiple access system. *IEEE Wireless Communications Letters*, *5*(5), 532-535. doi: 10.1109/LWC.2017.2665470

Wang, K., Liu, Y., Ding, Z., Nallanathan, A., & Peng, M. (2019). User association and power allocation for multi-cell non-orthogonal multiple access networks. *IEEE Transactions on Wireless Communications*, *18*(11), 5284-5298. doi: 10.1109/TWC.2019.2935433

Wu, G., Zheng, W., Xiong, W., Li, Y., Zhuang, H., & Tan, X. (2021). A novel low-complexity power allocation algorithm based on the NOMA system in a low-speed environment. *Digital Communications and Networks*, *7*(4), 580-588. doi: 10.1016/j.dcan.2021.07.001

Xu, P., & Cumanan, K. (2017). Optimal power allocation scheme for non-orthogonal multiple access with a-fairness. *IEEE Journal on Selected Areas in Communications*, *35*(10), 2357-2369. doi: 10.1109/JSAC.2017.2729780

Yang, M. J., & Hsieh, H. Y. (2015). Moving towards non-orthogonal multiple access in next-generation wireless access networks. In *2015 IEEE International Conference on Communications (ICC)*, pp. 5633–5638. doi: 10.1109/ICC.2015.7249220

Yu, W., Jia, H., & Musavian, L. (2021). Joint adaptive M-QAM modulation and power adaptation for a downlink NOMA network. *IEEE Transactions on Communications*, *70*(2), 783-796. doi: 10.1109/TCOMM.2021.3124947

**Yakov Kryukov**
Tomsk State University of Control Systems and Radioelectronics, Tomsk,
Russian Federation.
kryukov.tusur@gmail.com
ORCID 0000-0002-4115-9080

**Dmitriy Pokamestov**
Tomsk State University of Control Systems and Radioelectronics, Tomsk,
Russian Federation.
dmaltomsk@mail.ru
ORCID 0000-0002-9405-4573

**Andrey Brovkin**
Tomsk State University of Control Systems and Radioelectronics, Tomsk,
Russian Federation.
brovkintomsk@yandex.com
ORCID 0000-0003-1458-2008

**Artem Shinkevich**
Tomsk State University of Control Systems and Radioelectronics, Tomsk,
Russian Federation.
a.shinkevich00@gmail.com
ORCID 0000-0002-0174-9158

**Georgiy Shalin**
Tomsk State University of Control Systems and Radioelectronics, Tomsk,
Russian Federation.
shalingn1120@gmail.com
ORCID 0000-0001-5015-599X